

# CD36 homolog divergence is responsible for the selectivity of carotenoid species migration to the silk gland of the silkworm *Bombyx mori*<sup>S</sup>

Takashi Sakudoh,<sup>1,\*</sup> Seigo Kuwazaki,<sup>†</sup> Tetsuya Iizuka,<sup>§</sup> Junko Narukawa,<sup>†</sup> Kimiko Yamamoto,<sup>†</sup> Keiro Uchino,<sup>§</sup> Hideki Sezutsu,<sup>§</sup> Yutaka Banno,<sup>\*\*</sup> and Kozo Tsuchida<sup>1,\*</sup>

Division of Radiological Protection and Biology,<sup>\*</sup> National Institute of Infectious Diseases, Shinjuku Tokyo 162-8640, Japan; Insect Genome Research Unit<sup>†</sup> and Transgenic Silkworm Research Unit,<sup>§</sup> National Institute of Agrobiological Sciences, Tsukuba Ibaraki 305-8634, Japan; and Institute of Genetic Resources,<sup>\*\*</sup> Kyushu University, Fukuoka Fukuoka 812-8581, Japan

**Abstract** Dietary carotenoids are absorbed in the intestine and delivered to various tissues by circulating lipoproteins; however, the mechanism underlying selective delivery of different carotenoid species to individual tissues remains elusive. The products of the *Yellow cocoon (C)* gene and the *Flesh (F)* gene of the silkworm *Bombyx mori* determine the selectivity for transport of lutein and  $\beta$ -carotene, respectively, to the silk gland. We previously showed that the *C* gene encodes Cameo2, a CD36 family member, which is thought to function as a transmembrane lipoprotein receptor. Here, we elucidated the molecular identity of the *F* gene product by positional cloning, as SCRB15, a paralog of Cameo2 with 26% amino acid identity. In the *F* mutant, SCRB15 mRNA structure was severely disrupted, due to a 1.4 kb genomic insertion in a coding exon. Transgenic expression of SCRB15 in the middle silk gland using the binary GAL4-UAS expression system enhanced selective  $\beta$ -carotene uptake by the middle silk gland, while transgenic expression of Cameo2 enhanced selective lutein uptake under the same GAL4 driver.<sup>□</sup> Our findings indicate that divergence of genes in the CD36 family determines the selectivity of carotenoid species uptake by silk gland tissue and that CD36-homologous proteins can discriminate among carotenoid species.— Sakudoh, T., S. Kuwazaki, T. Iizuka, J. Narukawa, K. Yamamoto, K. Uchino, H. Sezutsu, Y. Banno, and K. Tsuchida. **CD36 homolog divergence is responsible for the selectivity of carotenoid species migration to the silk gland of the silkworm *Bombyx mori*.** *J. Lipid Res.* 2013. 54: 482–495.

**Supplementary key words**  $\beta$ -carotene • carotenoid absorption • carotenoid transport • cocoon color • lutein • positional cloning • SR-BI

This work was supported by the Teimei Empress Memorial Foundation (Japan), the Futaba Electronics Memorial Foundation (Japan), and JSPS KAKENHI Grant 21380045, 22770138 (Japan). Funding was also received from the Insect Technology Project of the Ministry of Agriculture, Forestry, and Fisheries (Japan) and the National Bioresource Project (Silkworm) of the Ministry of Education, Culture, Sports, Science, and Technology (Japan). The authors declare no competing financial interests.

Manuscript received 29 September 2012 and in revised form 4 November 2012.

Published, JLR Papers in Press, November 16, 2012

DOI 10.1194/jlr.M032771

Carotenoids are a group of more than 600 compounds that consist of hydrophobic pigments, with a central chain of conjugated double bonds (Fig. 1A) (1). Animals appear to be incapable of synthesizing these molecules, although they can chemically modify certain types (2). Thus, carotenoids must be acquired from dietary sources and transported to target tissues where they perform their diverse physiological functions (3–7).

Carotenoids are transported through the circulation in associated with lipoproteins. Interestingly, their uptake by tissues is often a selective process (*i.e.*, individual tissues tend to acquire only specific carotenoid species). For example, the human macula in the retina acquires lutein and zeaxanthin, to the exclusion of other carotenoids, such as  $\alpha$ -carotene,  $\beta$ -carotene, and lycopene (8). Selective transport of specific carotenoids is important, as molecular properties (*e.g.*, manifesting the optical absorption spectrum, provitamin A activity, and antioxidant activity) vary among the carotenoid species. While several carotenoid-binding proteins with differential carotenoid species affinities have recently been identified (9), the molecular genetic mechanism underlying the selectivity for the transport of carotenoid species to the relevant tissue has remained elusive.

The domesticated silkworm, *Bombyx mori*, offers a model system to study the transport selectivity of carotenoid species to target tissues (Fig. 1B, C). Wild-type larvae feed on mulberry leaves that are rich in lutein and  $\beta$ -carotene.

Abbreviations: BAC, bacterial artificial chromosome; *C*, *Yellow cocoon*; Cameo2, *C* locus-associated membrane protein homologous to a mammalian HDL receptor 2; EGFP, enhanced green fluorescent protein; *F*, *Flesh*; rpL3, ribosomal protein L3; RT, reverse transcription; SNP, single nucleotide polymorphism; SR-BI, scavenger receptor class B type I; UAS, upstream activating sequence; V0, day 0 of the fifth instar; W0, day 0 of the wandering stage.

<sup>1</sup>To whom correspondence should be addressed.

e-mail: sakudoh@nih.go.jp (T.S.); kozo@nih.go.jp (K.T.)

<sup>S</sup>The online version of this article (available at <http://www.jlr.org>) contains supplementary data in the form of one figure and three tables.



The *C* gene product was previously identified as *Cameo2*, a transmembrane protein-encoding gene belonging to the CD36 family, which is found in species ranging from mammals to insects (17). Some CD36 family proteins, such as the mammalian SR-BI and the fruit fly *NinaD*, have been implicated in cellular uptake of carotenoids (3–7). SR-BI also functions as a lipoprotein receptor and facilitates cellular uptake of cholesteryl ester from high-density lipoproteins (18).

In this study, we obtained genetic evidence that the *F* gene encodes *SCRBI5*, another member of the CD36 family.

## EXPERIMENTAL PROCEDURES

### Silkworms

Nontransgenic silkworm strains used in this study were preserved in the silkworm stock center at Kyushu University, Fukuoka, Japan, and the Genetic Resources Conservation Research Unit of the National Institute of Agrobiological Sciences, Ibaraki, Japan. The larvae were reared on mulberry leaves. The transgenic strains were produced and maintained in the Transgenic Silkworm Research Unit, National Institute of Agrobiological Sciences, Ibaraki, Japan. Larvae were reared on an artificial diet derived from mulberry leaves until the fourth instar, and on mulberry leaves during the fifth instar. The first days corresponding to the developmental stages of the fourth to fifth larval ecdysis, and wandering, a characteristic behavior with enhanced locomotory activity just prior to the commencement of the spinning of cocoons, were designated as V0 and W0, respectively. In this article, we designate the strain w06 with an  $F/+^F$  genotype as “w06F” for clarity.

### Mapping of the *F* gene using single nucleotide polymorphisms

In a previous crossing, during positional cloning of the *C* gene (17), we used strain c11 that is homozygous for the dominant *C* allele (wild-type allele) of the *C* gene and strain number 925 that is homozygous for the recessive  $+^C$  allele (mutant allele) of the *C* gene. As strain c11 and number 925 were also homozygous for the dominant *F* allele (wild-type allele) of the *F* gene and the recessive  $+^F$  allele (mutant allele) of the *F* gene, respectively, the BF1 progeny produced cocoons in which the appearance was divided into the following four colors according to the combination of the alleles of the *C* and the *F* genes: *i*) deep yellow, derived from the genotype [*C*, *F*] ( $C/+^C$ ,  $F/+^F$ ); *ii*) light yellow, derived from the genotype [*C*,  $+^F$ ] ( $C/+^C$ ,  $+^F/+^F$ ); *iii*) flesh, derived from the genotype [ $+^C$ , *F*] ( $+^C/+^C$ ,  $F/+^F$ ); and *iv*) white, derived from the genotype [ $+^C$ ,  $+^F$ ] ( $+^C/+^C$ ,  $+^F/+^F$ ) (supplementary Fig. 1).

After the visual assessment of the cocoon colors, genomic DNA was extracted from pupae in cocoons and used to map the *C* gene. In the BF1 individuals, there were no discrepancies between the single nucleotide polymorphism (SNP) marker pattern and cocoon color phenotype for the *C* gene. Subsequently, we used the BF1 progeny with the flesh-colored [ $+^C$ , *F*] and white [ $+^C$ ,  $+^F$ ] cocoons to map the *F* gene. We did not use [*C*, *F*] and [*C*,  $+^F$ ] because rigorous discrimination between individuals with these genotypes was difficult.

For *F* gene mapping, 16 SNP markers previously reported on chromosome 6, and 11 new SNP markers were used. The PCR primers for the SNP markers are listed in supplementary Table I or were published previously (19). PCR products were treated with ExoSAP-It (USB Corp., Cleveland, OH) and subjected to direct sequencing.

Analysis of 789 BF1 individuals by SNP genotyping indicated that 9 individuals had been misjudged by their cocoon colors; 8 BF1 individuals whose cocoons were judged to be white were in fact heterozygous for the SNP markers F-090703-03, F-100222-3-3, 06-013, F-100222-7-2, F-100222-8-1, and 06-011; and 1 BF1 individual whose cocoon had been judged to be flesh-colored was in fact homozygous for these markers (supplementary Table II). We therefore omitted these 9 individuals from Fig. 2 for the sake of simplicity. Even if these 9 individuals were taken into consideration,  $\log_{10}$  of the odds (LOD) scores for the SNP markers Bm\_scaf111-1, F-100222-3-3, 06-013, and Bm\_scaf111-4 were calculated to exceed 200, strongly supporting the linkage between these SNP markers and the *F* locus.

To determine the sequence of BAC clone 055\_A23, derived from the genomic DNA of strain p50, shotgun sequencing data obtained with a Roche 454 DNA sequencer by Hokkaido System Science Ltd. (Sapporo, Hokkaido, Japan) were combined with sequence data from the silkworm genome database KAIKObase (URL: [sgp.dna.affrc.go.jp/KAIKObase/](http://sgp.dna.affrc.go.jp/KAIKObase/)) (20).

### Quantification of transcripts by quantitative PCR

Total RNA was isolated from tissues as described previously (17). Single-stranded cDNAs from various tissue samples were synthesized from total RNAs with Superscript III reverse transcriptase (Invitrogen, Carlsbad, CA) and oligo-dT primer and were then treated with RNaseH (Takara, Kyoto, Japan). Quantification of transcripts was carried out by quantitative PCR using the cDNAs as templates with LightCycler FastStartDNA MasterPLUS SYBR Green I reagent (Roche, Mannheim, Germany) and a LightCycler DX400 thermocycler (Roche).

The primer pairs used for the detection of *SCRBI4*, *SCRBI1*, *SCRBI5*, *SCRBI2*, *SCRBI3*, and *rpL3* were Primer14-7 (5'-TGAAGAAGCTGAAGAAATGAGGTA-3') and Primer14-6 (5'-AAGGCTAGTTGAGGAAAGTAGGAG-3'), Primer11-3 (5'-GAAGCACCAGTAATCAGGTTTACAC-3') and Primer11-2 (5'-GGTTCATTAAAGTCGACACAGTC-3'), Primer15-3 (5'-GAGAAGATGTTTCGAGAAACAATCTTTGC-3') and Primer15-2 (5'-TCGAACAGTTTTGGATCAGCATCC-3'), Primer12-3 (5'-CCATAACGCACCATCGTATACAG-3') and Primer12-2 (5'-TTCCCACCCTCATTTCTGTAAATGG-3'), Primer13-5 (5'-AGATCCACCTCTTCAACTACACAA-3') and Primer13-4 (5'-TACCCTCATCGACTGTTATGTTTT-3'), and Primer-rpL3-real-cDNA1 (5'-TTCCCGAAAGACGACCCTAG-3') and Primer-rpL3-real-cDNA2 (5'-CTCAATGTATCCAACAACACCGAC-3'), respectively.

Serial dilutions of plasmids containing the cDNA sequences were used as copy-number standards. Transcript levels of the genes other than *rpL3* were normalized to the level of the *rpL3* transcript in the same samples, as described previously (21).

### Comparison of *SCRBI1*, *SCRBI5*, and *SCRBI2* cDNA sequences between individuals carrying the *F* allele and those carrying the $+^F$ allele

For *SCRBI1* and *SCRBI2*, full-length cDNA sequences from strain p50 were obtained from the KAIKObase database. *SCRBI1* and *SCRBI2* were amplified from the middle silk gland of each of strains c44 (*F/F*) and w06 ( $+^F/+^F$ ) via reverse transcription (RT)-PCR and were then directly sequenced. The PCR primers used for *SCRBI1* were Primer11-5 (5'-GCAATCATCTCACAACCCTTTACTG-3') for the 5'-UTR and Primer11-4 (5'-GAGGCACTATCTAAGGCCAGGTTTA-3') for the 3'-UTR. For *SCRBI2*, we used Primer12-7 (5'-GCTAGCTAGTGCCTTTTCAATTCTA-3') for the 5'-UTR and Primer12-4 (5'-GCGAGTACACAGACTGACAAACTGA-3') for the 3'-UTR.

For *SCRBI5*, the cDNA sequence containing the full-length coding sequence from the *F* allele was determined from strain c44 (*F/F*). First, a partial *SCRBI5* cDNA fragment was amplified



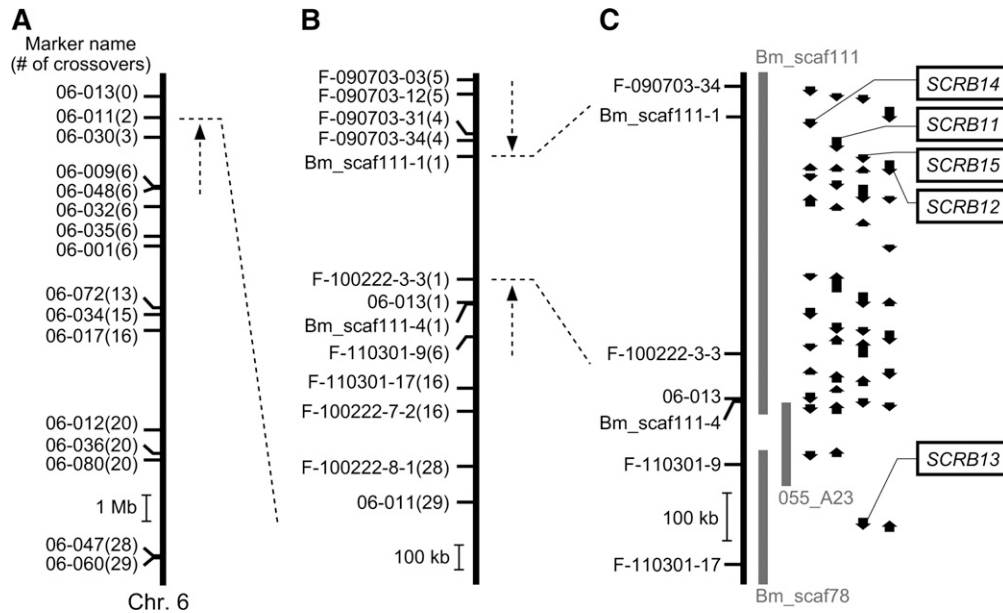


**Fig. 2.** Mapping of the *F* gene on chromosome 6. (A) Rough mapping using 58 individuals. Small horizontal lines on the vertical bars of chromosome 6 denote the positions of crossover events, showing the name of the SNP marker and the number of recombinants. (B) Fine mapping using 789 individuals. Nine individuals that were considered to have been misjudged for their cocoon colors were omitted from the number of recombinants (see Experimental Procedures for details). (C) Physical map of chromosome 6 near the *F* locus harboring the predicted *F* gene. Vertical arrows indicate the orientation and relative size of the putative genes predicted by the China gene model in the silkworm genome database KAIKObase (20). Sequence of BAC clone 055\_A23 was determined in this study to fill the gap between Bm\_scaf111 and Bm\_scaf78. No sequences homologous to Cameo2 were found in 055\_A23. *SCRBI1–15* were named in previous reports (17, 49).

from the middle silk gland via RT-PCR with the primer pair Primer15-1 (5'-GATAAGAACGTACTACTATCGCATGG-3') and Primer15-2 (5'-TCGAACAGTTTTGGATCAGCATCC-3'), both of which were designed based on the predicted *SCRBI5* fragment sequence (BGIBMGA013438 in the China gene model in the KAIKObase). The sequence of amplified fragments was determined by direct sequencing. Subsequently, four more primers, Primer15-11 (5'-CACCTATGAAGGCATGGCATAACCCACCG-3'), Primer15-13 (5'-CACGGCAATAAGACGTCGGAATACGGCC-3'), Primer15-8 (5'-CCTTTAGGGCAAGCCCCCTTAACATCGC-3'), and Primer15-10 (5'-GCCCCCTTTGATAATCCCATGGGCAAACC-3'), were designed based on the determined partial sequence.

The 5'- and 3'-ends of the *SCRBI5* sequence were obtained via rapid amplification of cDNA ends (RACE) using a SMART RACE cDNA amplification kit (Clontech, Mountain View, CA) with Primer15-10 for the first 5'-RACE product, Primer15-8 for the nested 5'-RACE product, Primer15-11 for the first 3'-RACE product, and Primer15-13 for the nested 3'-RACE product. The determined sequence was then combined to obtain the full-length *SCRBI5* cDNA sequence from strain c44 (*F/F*).

*SCRBI5* cDNA sequences from strain w06 ( $+^F/+^F$ ) were amplified from the middle silk gland via RT-PCR with two primer pairs, Primer15-5 (5'-GATATATGAATTTTCGCAAAAGAGACTAAG-3') for the 5'-UTR and Primer15-12 (5'-TCAATGCAGTCAATCCTTAC-3') for the 3'-UTR, and Primer15-23 (5'-ATAGGGAGCCGGAGTAATGAGGTA-3') and Primer15-22 (5'-CAGACTCAGGGTGGAGTCGAGTAT-3') for the coding exon, and directly sequenced. The *SCRBI5* cDNA sequence from strain w06 ( $+^F/+^F$ ) was identical to that from strain c44 (*F/F*) except for a splicing out of exon 6 or a 1.4 kb insertion into exon 6 (for details, see Results). The *SCRBI5* cDNA sequence from strain e09 ( $+^F/+^F$ ) was amplified via RT-PCR with the primer pair Primer15-5 and Primer15-12, and directly sequenced. The *SCRBI5* cDNA

sequence from strain e09 ( $+^F/+^F$ ) was identical to that from strain w06 ( $+^F/+^F$ ).

### Northern blotting analysis

A  $^{32}$ P-labeled riboprobe was synthesized from a plasmid containing both the 3' part (621 bp) of the coding sequence and the 5' part (39 bp) of the 3'-UTR of *SCRBI5*. No repetitive sequence was found in the insert of this plasmid. Total RNA was electrophoresed on 1% agarose gels containing formaldehyde and was then transferred onto Hybond N<sup>+</sup> membrane (GE Healthcare UK, Buckinghamshire, England). Hybridization was performed with Ultrahyb (Ambion, Austin, TX).

### *SCRBI5* genomic sequence analysis

As a part of the *SCRBI5* genomic sequence, including exons 4–6, was absent from the publicly available silkworm genome sequence data (22), we determined the sequence of genomic fosmid clone RO0299-D04, derived from strain p50 by a shotgun method (23, 24), to reveal the overall genomic structure of *SCRBI5*.

To compare the genomic sequence of exon 6 between the *F* and the  $+^F$  alleles, the genomic sequence of each of strains c44 (*F/F*), w06 ( $+^F/+^F$ ), and e09 ( $+^F/+^F$ ) was amplified via PCR with the primer pair Primer15-25 (5'-ATCGCCCGTCTTCATTTCGTAATATC-3') and Primer15-20 (5'-TAAAATATACGAGACCAGGCACCAA-3') and then directly sequenced. The sequences amplified from strain w06 ( $+^F/+^F$ ) and strain e09 ( $+^F/+^F$ ) were identical.

For genotyping by PCR, the following primers were used in addition to those described above: Primer15-18 (5'-ATTCTTCAGGAACAAACACAGATCG-3'), Primer15-21 (5'-AATTTTCGTCTTGCCAATGGAAGTAT-3'), Primer15-24 (5'-CGTAACACCAAGGT-TTTGGAAGGAA-3'), Primer15-25 (5'-ATCGCCCGTCTTCATTTCGTAATATC-3'), Primer15-30 (5'-GAATGAAGACGGCCGATGAT-3'), and Primer15-31 (5'-TGCCTGGTCTCGTATATTTTAACAC-3').

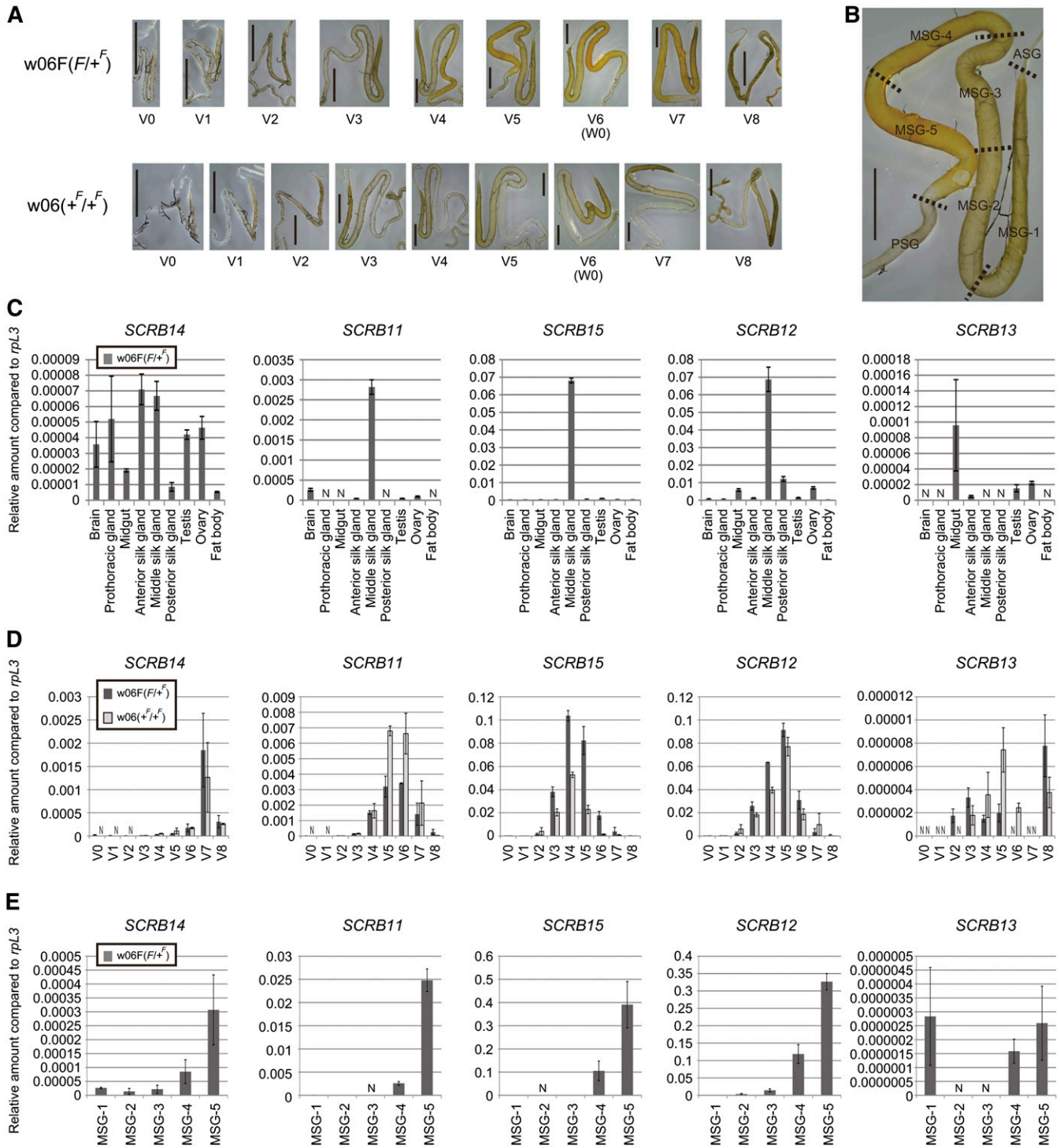


**Fig. 3.** Expression analysis of the *F* gene candidates by quantitative RT-PCR. (A) Developmental changes in carotenoid pigmentation associated with the *F* allele in the silk gland during the fifth larval instars. From day 6 of the fifth larval instar [V6 (W0)], larvae spat silk for cocoon formation, resulting in a decrease of carotenoid pigmentation and degradation of the silk gland. The silk gland image from strain w06 ( $+^F/+^F$ ) at day 7 of the fifth larval instar (V7) was made by combining two photographs. Scale bar: 0.5 cm. (B) Spatial difference in carotenoid pigmentation of the silk gland. The silk gland depicted from strain w06F ( $F/+^F$ ) at the V5 stage is the same as in (A). Definition of regions in the silk gland is the same as described previously (17): ASG, anterior silk gland; MSG-1–5, middle silk gland-1–5; PSG, posterior silk gland. (C–E) Quantitative RT-PCR analysis of expression levels of the *F* gene candidates, *SCR14*, *SCR11*, *SCR15*, and *SCR12*. *SCR13*, which was located outside of the delimited region for the *F* locus (Fig. 2C), was also included in the analysis. (C) Tissue distribution of the expression of the *F* gene candidates on day 5 of the fifth larval instar (V5). (D) Developmental expression profile in the middle silk gland of the fifth instar larvae. (E) Spatial expression analysis of the middle silk gland at the V5 stage. The vertical axis shows the transcript levels of each gene normalized to the level of the reference gene *ribosomal protein L3* (*rpl3*) (mean, SE;  $n = 3$ ). As the efficiency of reverse transcription could differ among target genes, the value of the vertical axis of a particular gene could not necessarily be compared with the value of that of the other genes. Male larvae were used for the data in this figure, except for ovary data. N, not detected.

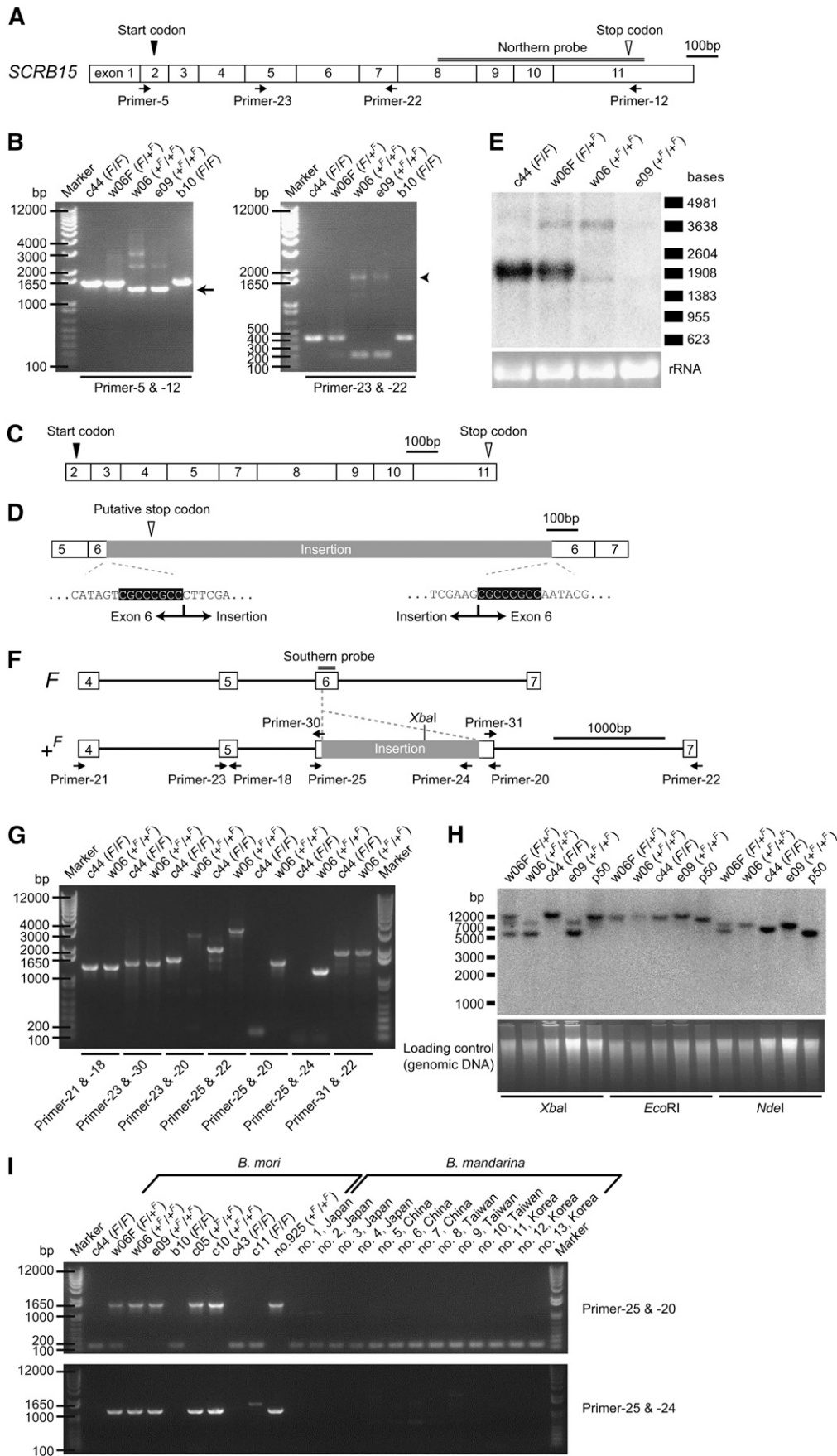


**Fig. 4.** Genomic insertion in an *SCRBI5* coding exon of the *F* mutant. (A) Schematic *SCRBI5* mRNA structure from strain c44, which is homozygous for the *F* allele. Exon boundaries were determined based on the genomic sequence database (for exons 1–3 and 7–11) (20) and our own genomic sequence data (for exons



For Southern blotting analysis, a digoxigenin-labeled DNA probe for *SCRBI5* exon 6 was amplified from a cDNA-containing vector by PCR using the primer pair Primer15-25 and Primer15-20. The hybridization and detection procedures with this probe were described previously (25).

### Silkworm transgenesis

Transgenic *SCRBI5* expression using the binary GAL4/upstream-activating sequence (UAS) system (26) was performed as described previously (17). To construct the effector vector, pBacMCS[UAS-*SCRBI5*-3xP3-EGFP], *SCRBI5* was amplified by RT-PCR from the middle silk gland of strain c44 (*F/F*) with Primer15-17 (5'-ATGCACTAGTTTTTCGCAAAAGAGACTAAG-3') for the 5'-UTR and Primer15-14 (5'-ATGCACTAGTCAATGCAGTCAATCCTTACA-3') for the 3'-UTR, both of which contain an *SpeI* site. The amplified fragment was digested with *SpeI* and ligated into a pBacMCS[UAS-3xP3-EGFP] vector (27), which was previously digested with *BlnI*. For the effector strains, the effector construct and the helper plasmid pHA3PIG (28) were injected into preblastoderm embryos of the strain w1-pnd-925, a nondiapausing strain with the phenotype of yellow hemolymph and white cocoons (17). The existence of the transgene was identified by the fluorescence in the eye, EGFP for *UAS-SCRBI5* and DsRed2 for *SerI-GAL4* (29). Individuals exhibiting colorless hemolymph in the larval stage, which had colorless silk glands and produced white cocoons, were not used to examine the color phenotype or carotenoid composition of the middle silk gland and cocoons.

### Analysis of carotenoid composition

Larval hemolymph was collected into an Eppendorf tube, frozen in liquid nitrogen, and stored at  $-70^{\circ}\text{C}$  until use. Thawed hemolymph was centrifuged at 800 *g* for 5 min to remove hemocytes. Twenty microliters of the supernatant was transferred into a glass tube with 3.0 ml of dimethyl sulfoxide (DMSO), mixed, and sonicated at  $50\text{--}60^{\circ}\text{C}$  for 30 min. The middle silk gland was frozen in liquid nitrogen and broken into fine pieces; some of these pieces (20–170 mg) were then transferred into a glass tube with 3.0 ml of DMSO, mixed, and sonicated at  $50\text{--}60^{\circ}\text{C}$

for 30 min. A cocoon (6–14 mg) was cut into small pieces of less than 1 mm width using scissors; these pieces were then transferred into a glass tube with 2.0 ml of DMSO, mixed, and sonicated at  $50\text{--}60^{\circ}\text{C}$  for 30 min. After collection of the extracts, residual cocoon pieces were extracted twice more with 2.0 ml of DMSO, and the resulting three extracts were pooled. After filtration through a polyvinylidene difluoride membrane, the extracted carotenoid composition was analyzed by high-performance liquid chromatography (HPLC). A reverse-phase column (DOCOSIL SP100 [ $6 \times 250$  mm]; Senshu Kagaku, Tokyo, Japan) was used under the following conditions: mobile phase, isocratic solvent, 70% methanol, and 30% ethyl acetate; room temperature; flow rate, 2 ml/min; and detection, 445 nm. Carotenoid standards were purchased from Sigma (St. Louis, MO).

### Data deposition

The cDNA sequence of *SCRBI1* from c44 (*F/F*), and of that from w06 ( $+^F/+^F$ ), the cDNA sequence of *SCRBI2* from c44 (*F/F*), and of that from w06 ( $+^F/+^F$ ), the cDNA sequence of *SCRBI5* from strain c44 (*F/F*), the sequence of the insertion in exon 6 of *SCRBI5* from strain w06 ( $+^F/+^F$ ), the sequence of the BAC clone 055\_A23, and the sequence of genomic fosmid clone RO0299-D04 have been deposited in GenBank under accession nos. AB742534, AB742535, AB742536, AB742537, AB742538, AB742539, AB742540, and AB742541, respectively.

## RESULTS

### Mapping of the *F* gene on chromosome 6 of the silkworm

To specify a candidate genomic region for the *F* gene, we performed genetic linkage analysis using SNP markers (19) and the *B. mori* genome sequence (22). Using 58 BF1 individuals, the *F* locus was roughly mapped on chromosome 6, on which the *F* gene lies (30, 31). The *F*-linked region was narrowed to an end of chromosome 6, bounded by the SNP marker 06-011 (Fig. 2A).

4–6). (B) RT-PCR analysis of the *SCRBI5* mRNA structure from the middle silk gland. PCR primer positions were as depicted in (A). The length of PCR products differed between the *F* and  $+^F$  allele. (C) The *SCRBI5* mRNA structure obtained from a shorter band from strain w06 ( $+^F/+^F$ ) [arrow in (B)]; in this case, exon 6, consisting of 201 base pairs, had been spliced out. (D) Another mRNA structure of *SCRBI5* obtained from a longer band from strain w06 ( $+^F/+^F$ ) [arrowhead in (B)]. An insertion of 1.4 kb was present in exon 6. Duplication of eight bases occurred at the insertion site (highlighted). A putative stop codon was present in this insertion. (E) Northern blotting analysis of *SCRBI5* in the middle silk gland on day 3 of the fifth larval instar [for strains c44 (*F/F*) and e09 ( $+^F/+^F$ )] or day 4 of the fifth larval instar [for strains w06F (*F/+^F*) and w06 ( $+^F/+^F$ )]. For both strains w06 ( $+^F/+^F$ ) and e09 ( $+^F/+^F$ ), a longer band, which may correspond to the mRNA containing the 1.4 kb insertion, and a shorter band, which may correspond to the mRNA lacking the 201 base pair exon 6, were detected. The expression of the transcript from strain e09 ( $+^F/+^F$ ) was lower than that of the transcript from strain w06 ( $+^F/+^F$ ), which was confirmed by quantitative RT-PCR analysis (data not shown). (F) Schematic genomic structure of *SCRBI5*. The structure, except the insertion in exon 6, was based on the data from strain p50. (G) Genotyping of *SCRBI5* by genomic PCR. Positions of PCR primers are as illustrated in (F). The intron between exons 5 and 6 in both strain c44 and w06 would be longer than that in strain p50. (H) Southern blotting analysis of *SCRBI5*. Genomic DNA completely digested with *XbaI*, *EcoRI*, or *NdeI* was used. The position of the Southern probe is double-lined in (F). The genomic insertion in the  $+^F$  allele contained one *XbaI* recognition site, as indicated in (F). No *EcoRI* or *NdeI* recognition sites were found within the insertion. Predicted *XbaI* fragment sizes were 11.6 kb for the *F* allele and 7.7 kb (weaker) and 5.3 kb (stronger) for the  $+^F$  allele. Predicted *EcoRI* fragment sizes were 10.9 kb and 12.3 kb for the *F* and  $+^F$  alleles, respectively. Predicted *NdeI* fragment sizes are 6.4 kb and 7.8 kb for the *F* and  $+^F$  alleles, respectively. (I) Genotyping of *SCRBI5* by genomic PCR in multiple strains of *B. mori* and multiple individuals of *B. mandarina*, the putative wild ancestor of *B. mori* (33). Details of the geographical location of the sampling area of *B. mandarina* are as described previously (50). The different band from strain c11 obtained with Primer-25 and Primer-24 was an artifact unrelated to *SCRBI5* that was amplified with Primer-24 as both sense and antisense primers (data not shown).

**A**

```

SCRB15 1: MSSIFKVSPPQELIKRRLLLALSGLAFLLLISSIALILTDPMMWAIKYKFRLANGSILHEL 60
Cameo2 1: -----MRCGLLRWRSLLWICGGALLALSFAVAALTWGAITDSAFGSQLALIPDSRSF 51

SCRB15 61: LSSEMEGG--RFAVILFNITNPDRELSCEDFYLKLDVGGFTTLYEYRTHSELQDFRDAV 118
Cameo2 52: MRWLEPDVPIFEIDYIMFNWNTNPPREPE-EKE--NFEETIGEYRYCEHRRHVNISWHPEHGT 108

SCRB15 119: MRYTTPRMRSVFVHEESIGNPEDIFLITMPNTPMLSAITMTIRSSPVFTIRNIYNIVARQYGSQ 178
Cameo2 109: IGYR-TLRSWVWDESSVGSQDDIITIDVITA-SAIYQARFS-GFIEQKLVSLTLTS-SQ 164

SCRB15 179: -PIVKL--AASKYTLW-GYKDFVITFANSLVPE----GLVYFNTTQIMDRLYDKNVHYRME 229
Cameo2 165: HTKVSVTARASEFLFFGYEDELINLAK-LMPASVRCGAPALDRFGWFFSRNNTDIDTGYME 223

SCRB15 230: LGTNDDDKFKIKRTHHYTRLHPSEVFFDESILTFNDTYEGMAYEPPMIGKNTPIINIFRLGI 289
Cameo2 224: VTSGTRDGLPG-QLLRWN--YQDHIFPYDGECSKLSGSGAGEYIERNLTEDSKLTMVYVPL 280

SCRB15 290: CKSFMETVYHGKNTSEYGFNAFVYKNEKMFEN-----NLIDVKGACPKG-VMDLSAGFY 342
Cameo2 281: CRTVMVEFVESGVQN-GLKYNKYEVNERSEDSSTSPENITCCKGCAWGSVMNVSACRF 339

SCRB15 343: GLPFGLSKGLLDADPKLDFRIKLPKDFPKHSHLVIEPKIGLTLETSSWISLANIFVGD 402
Cameo2 340: GSPAFITLPHFLHGDBALLDQVTCMNPDEPKHSFYFAVEPKLGVPIDVAGRFQFNIVYVEP 399

SCRB15 403: ITYNAEAKMFSNMLLTAHFKIKQPHLPSTATTALRMYITVPKALFITEILLMLSCLLL 462
Cameo2 400: SDHITLYENMPRLLEFVFWVECKAKIDPKT-ISELRTVIRGILDWGPTEFCACFAVVIALLV 458

SCRB15 463: LVYSAWLLHWKRVHKKQPTSEKELQISSRMANEPLMSYLTIN 504
Cameo2 459: TAITCCGTRKREYTRPHDLKPE-----YEKPKDEAEKLNPL- 494

```

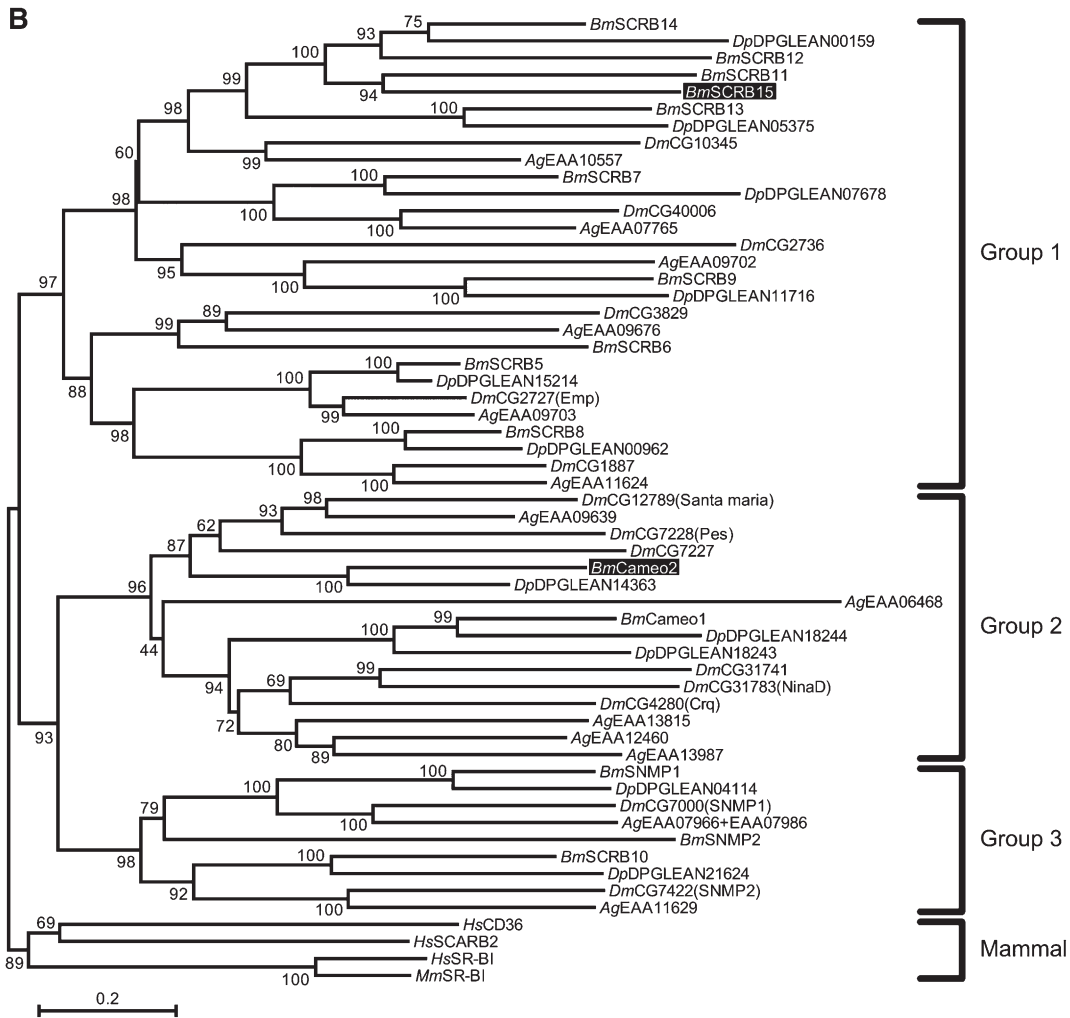


**Fig. 5.** Putative SCR15 amino acid sequence. (A) Alignment of putative amino acid sequences of SCR15 and Cameo2. Identical amino acid residues are boxed. Transmembrane helices predicted by TMHMM version 2.0 (35) are highlighted. N-Glycosylation consensus sites (N-X-S/T) and cysteine residues in the putative extracellular region, common features in CD36-related genes (36), are indicated by asterisks and bold type, respectively. (B) A neighbor-joining tree for SCR15 and other homologs from insects and mammals generated using MEGA5 software (51). SCR15 and Cameo2 are highlighted. The first two characters of the gene names represent their species: *Bm*, *B. mori*;



Next, novel primer sets were designed and fine mapping was performed with 789 BFI individuals. During the fine mapping, a BAC genomic DNA clone, 055\_A23, which bridges the gap between the two scaffolds, Bm\_scaf111 and the Bm\_scaf78, was sequenced since the *F*-linked region appeared to occur in this area. Consequently, the *F*-linked region was narrowed down to a 499 kb region between two SNP markers, Bm\_scaf111-1 and F-100222-3-3, both of which were on the same scaffold, Bm\_scaf111 (Fig. 2B and supplementary Table III). Twenty-six genes were predicted to lie within the narrowed region of genomic DNA, based on the China gene model of the silkworm genome database, KAIKObase (20) (Fig. 2C). Among these genes, four (i.e., *SCRBI4*, *SCRBI1*, *SCRBI5*, and *SCRBI2*) belong to the *CD36* gene family; that is, they are paralogs of *Cameo2*. The function of the *F* gene is similar to that of the *C* gene, despite its unique carotenoid species selectivity. Therefore, we considered these four genes to be possible *F* gene candidates. No other *Cameo2* paralogs, other than *SCRBI3*, were found within the genomic sequence of chromosome 6, including the BAC clone 055\_A23 (Fig. 2C).

### Expression analysis of *Cameo2* paralogs near the *F* locus

Cellular uptake of  $\beta$ -carotene in the middle silk gland, associated with the *F* gene, occurs in a spatiotemporally controlled manner (10) (Fig. 3A, B). To examine its relationship to  $\beta$ -carotene uptake, we examined the expression profiles of the *F* gene candidates with quantitative RT-PCR. *SCRBI3*, which lies outside of the *F*-linked region, was also included in the analysis for comparison. *SCRBI1*, *SCRBI5*, and *SCRBI2* exhibited a middle silk gland-specific expression pattern in final instar larvae possessing the *F* allele, the dominant wild-type allele of the *F* gene (Fig. 3C). Expression levels of these three genes in the middle silk gland of the strain with the *F* allele were higher in the mid-stage of the final instar when  $\beta$ -carotene was extensively acquired by the middle silk gland (Fig. 3D). In the posterior portion of the middle silk gland, within which  $\beta$ -carotene mainly accumulates, the highest expression of these three genes was noted (Fig. 3E). In contrast, *SCRBI4* and *SCRBI3* expression levels were not specific to the middle silk gland (Fig. 3C) and were not well correlated with developmental changes in  $\beta$ -carotene uptake by the middle silk gland (Fig. 3D).

### Genomic insertion in a coding exon severely affects the *SCRBI5* mRNA structure in the *F* mutant

Next, the coding sequences of *SCRBI1*, *SCRBI5*, and *SCRBI2* were compared between the chromosome containing the *F* allele and that containing the  $+^F$  allele by RT-PCR and sequencing. *SCRBI1* and *SCRBI2* were well

conserved and did not show insertions, deletions, or premature stop codons, but they demonstrated four nonsynonymous substitutions in *SCRBI1* [i.e., Y19N [from tyrosine at amino acid position 19 in strain c44 (*F/F*) to asparagine in strain w06 ( $+^F/+^F$ )], I116N, D305E, and V454I]. In contrast, RT-PCR revealed that the *SCRBI5* coding sequence lengths were significantly different between these chromosomes (Fig. 4A, B). Sequencing of the smaller PCR product from strain w06 ( $+^F/+^F$ ) (Fig. 4B, arrow) revealed the absence of 201 base pairs in the coding sequence (Fig. 4C). These 201 base pairs perfectly corresponded to *SCRBI5* exon 6. Sequencing of the larger PCR product (Fig. 4B, arrowhead) identified an insertion of 1,400 base pairs in exon 6 (Fig. 4D). Although the insertion was not homologous to known transposable elements (32), a duplication of eight nucleotides was found at the insertion site (highlighted in Fig. 4D), which could be a sign of an insertion event. Northern blotting analysis (Fig. 4E) supported the structural difference in *SCRBI5* between the chromosome bearing the *F* allele and that bearing the  $+^F$  allele and revealed a decrease in *SCRBI5* expression in strains with the  $+^F$  allele, consistent with the results of quantitative RT-PCR analysis (Fig. 3D).

The genomic sequence of *SCRBI5* was also compared between the *F* and  $+^F$  allele (Fig. 4F–H); this revealed that the same insertion occurred in the genomic sequence of exon 6 of the  $+^F$  allele. Thus, likely due to this genomic insertion, *SCRBI5* exon 6 was either spliced out (Fig. 4C) or transcribed with the insertion (Fig. 4D), resulting in the absence of 67 amino acids or an unusual stop codon contained in the insertion sequence, respectively, in the *F* mutant.

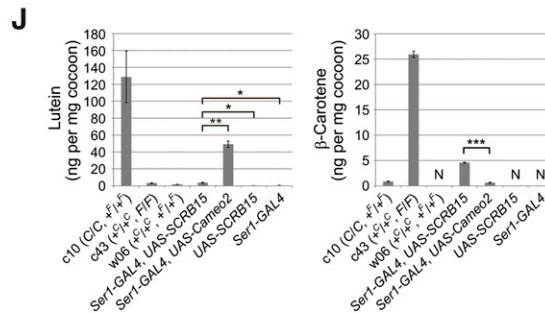
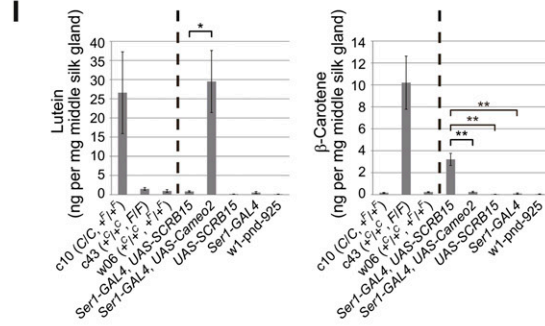
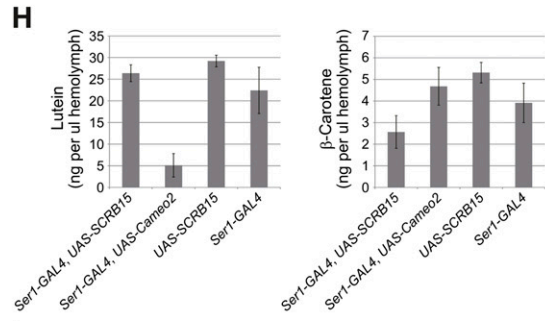
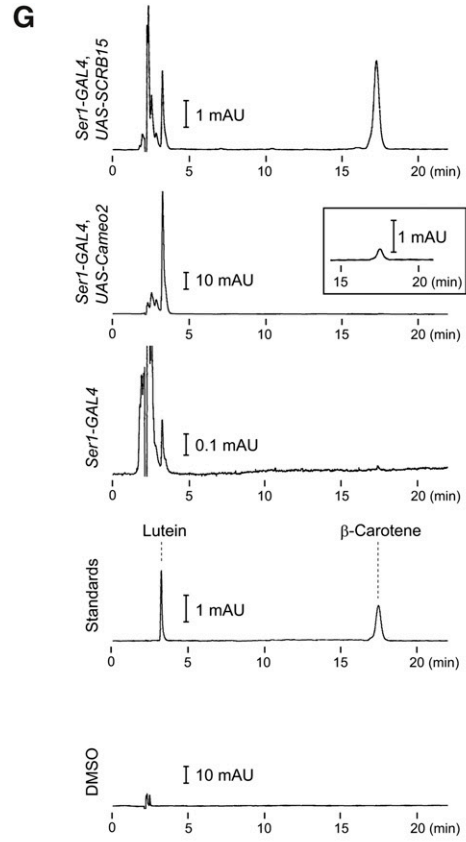
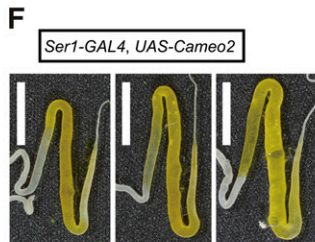
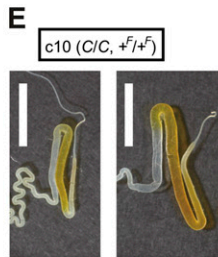
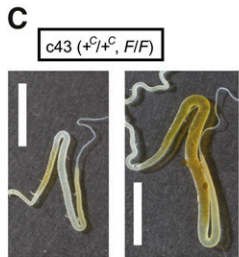
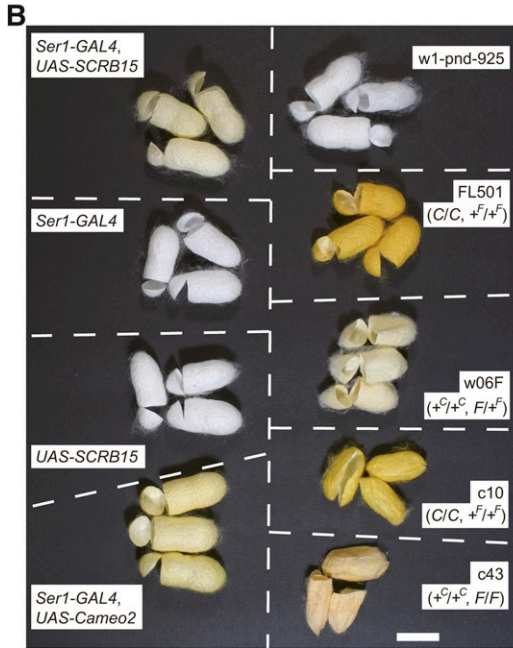
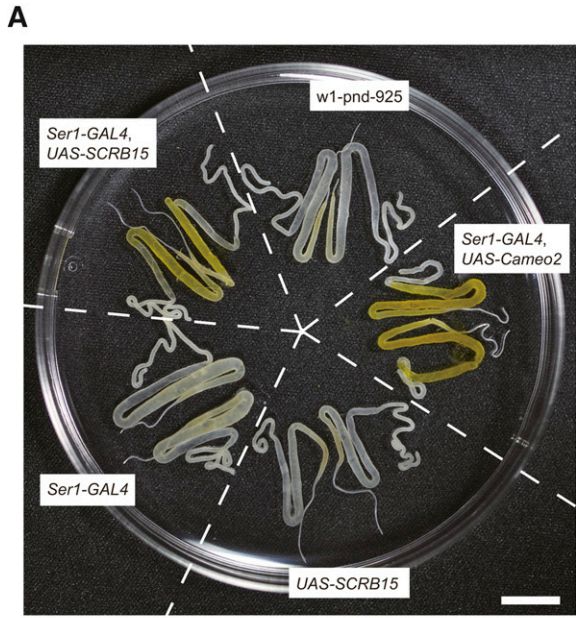
Genotyping of *SCRBI5* in multiple strains of *B. mori* and multiple individuals of *B. mandarina*, the putative wild ancestor of *B. mori* (33), indicated that the insertion occurred in every  $+^F$  allele-bearing individual from different strains of *B. mori*, but it was absent in *B. mandarina*, suggesting a common and single origin of the  $+^F$  allele (Fig. 4I). This origin could be associated with the previous categorization of *SCRBI5* (termed BGIBMGA013438) into the 354 protein-coding genes of the silkworm that represent good candidates for artificial selection during silkworm domestication, identified from a whole-genome analysis of approximately 16 million SNPs (34).

### Bioinformatic characterization of the *SCRBI5* sequence

*SCRBI5* was predicted to encode a 57.6 kDa protein composed of 504 amino acids; glycosylation at five N-glycosylation consensus sites was expected to increase the molecular weight of the protein (Fig. 5A). Its amino acid identity with *Cameo2* was 26%. Identical amino acid residues between *SCRBI5* and *Cameo2* were dispersed over the entire

---

*Dm*, *D. melanogaster*; *Ag*, *Anopheles gambiae*; *Dp*, *Danaus plexippus*; *Hs*, *Homo sapiens*; and *Mm*, *Mus musculus*. Numbers at nodes indicate the percentage of bootstrap values of 10,000 replicates. Groups are based on previous reports (39, 40). Although 21 homologs were found in the gene database of *Danaus plexippus* (38), only 11 of those more than 368 amino acids long were included in this tree; the other 10 homologs were shorter than 288 amino acids. DPGLEAN04114 of *Danaus plexippus* (accession number: EHJ78189) is composed of 1,801 amino acids, while the other CD36 homologs are approximately 500 amino acids. DPGLEAN04114 consists of an aldehyde oxidase-homologous sequence at the N-terminus and a CD36-homologous sequence, closely related to SNMP1, at the C terminus. Both aldehyde oxidase (52) and SNMP1 (53–55) are implicated in pheromone detection in insect olfactory neurons.





sequence, but there were fewer in the central section (residues 215–289 in *SCRB15*). TMHMM software (35) analysis suggested that *SCRB15* comprises a large extracellular loop, anchored to the plasma membrane on each side by transmembrane domains adjacent to short cytoplasmic N-terminal and C-terminal domains. The putative molecular mass, transmembrane topology, and multiple glycosylation sites of *SCRB15* are common to members of the CD36 family (36). The theoretical isoelectric point deduced from the primary amino acid sequences was somewhat different for the predicted extracellular loop of *SCRB15* (pH 7.8) and that of *Cameo2* (pH 5.0). While our previous analysis using the SignalP 3.0 program suggested that the first N-terminal helices of some of CD36 family proteins, including *Cameo2*, represented a signal peptide (17), analysis using the SignalP 4.0 program (37), a new software version designed to discriminate between signal peptides and transmembrane regions, suggested that the first N-terminal transmembrane helices of *SCRB15* and *Cameo2* are anchored to the membrane and are not signal peptides.

A phylogenetic tree of CD36 protein family members from mammals and insects, including the monarch butterfly *Danaus plexippus*, whose whole genome was recently reported (38), was constructed based on their primary amino acid sequences (Fig. 5B). As shown in previous studies (39, 40), the insect proteins could be divided into three groups, while mammalian proteins formed a single, distinct group. *SCRB15* and *Cameo2* were somewhat removed from each other and fell into groups 1 and 2, respectively. *SCRB11–15* formed a Lepidoptera-specific clade in group 1, suggesting that a small expansion may have occurred in the Lepidopteran lineage.

#### Enhancement of $\beta$ -carotene selective uptake into the middle silk gland by transgenic expression of *SCRB15*

To verify the function of *SCRB15* as a product of the *F* gene, we examined the restoration of  $\beta$ -carotene accumulation in the middle silk gland after transgenic expression of the *SCRB15* gene in a strain with the phenotype of the *F* mutant, using the binary *GAL4/UAS* system (26). Following transgenic expression of *SCRB15* in the middle silk gland by the *Ser1-GAL4* driver (29), pigmentation was observed in the middle silk gland (Fig. 6A). Cocoon pigmentation was also restored, although the color was not as intense as those of some nontransgenic strains (Fig. 6B).

We next focused on the region of pigmentation in the middle silk gland of the last larval instar. As mentioned before, pigmentation in the larvae bearing the *F* allele commences in the posterior part and spreads into the middle of the gland (Figs. 3A and 6C) (10), which likely reflects the expression pattern of *SCRB15* (Fig. 3E) and migration of liquid silk toward the anterior part of the silk gland. In contrast, pigmentation of the transgenic larvae, in which the *SCRB15* expression was driven by *Ser1-GAL4*, commenced from the middle part and spread into the posterior part of the gland (Fig. 6D). This pattern was concordant with the property of the *Ser1-GAL4* driver as monitored using the *UAS-EGFP* gene (29). On the other hand, the pigmentation pattern in larvae bearing the *C* allele commences from the middle part of the gland but spreads into the posterior region only minimally (Fig. 6E) (10), which likely reflects the middle-specific expression pattern of *Cameo2* (17). In the transgenic larvae, in which *Cameo2* expression was driven by *Ser1-GAL4*, pigmentation commenced from the middle and spread into the posterior part (Fig. 6F) (17), which is similar to what was observed in the *SCRB15* transgenic larvae but not larvae bearing the *F* or *C* allele. Overall, the pigmentation seemed to occur where *SCRB15* or *Cameo2* were expressed. These data suggest that carotenoid uptake by *SCRB15* or *Cameo2* do not require cofactors of which the expression is restricted to limited regions in the middle and posterior parts of the middle silk gland. It should be noted that the carotenoid-binding protein (CBP), which is an obligate cofactor of the products of both the *C* gene and the *F* gene for carotenoid transport into the middle silk gland (10, 12), is expressed from the middle to the posterior part of the middle silk gland (17, 41).

Carotenoid content of larval hemolymph, middle silk gland, and cocoons of the transgenic lines were analyzed by HPLC with a reverse-phase column (Fig. 6G–J). A decrease in  $\beta$ -carotene, but not lutein content, was observed in hemolymph of transgenic larvae expressing *SCRB15* (Fig. 6H). This may be due to selective uptake of  $\beta$ -carotene by the middle silk gland (Fig. 6I). Cocoons produced by the transgenic larvae expressing *SCRB15* selectively accumulated  $\beta$ -carotene (Fig. 6J). The  $\beta$ -carotene quantities did not reach the same level as in a strain bearing the *F* allele, which is consistent with observations regarding the color intensity of the cocoons (Fig. 6B).

**Fig. 6.** Restoration of selective  $\beta$ -carotene uptake by transgenic expression of *SCRB15*. (A) Silk glands of the *Ser1-GAL4/UAS-SCRB15* line, which expresses *SCRB15* in the middle silk gland from the binary *GAL4/UAS* system (26) with a *Ser1-GAL4* driver (29). The *Ser1-GAL4* line, the *UAS-SCRB15* line, and the w1-pnd-925 line are control lines that do not express *SCRB15*. The *Ser1-GAL4/UAS-Cameo2* line (17) expresses *Cameo2* and selectively accumulates lutein in the middle silk gland. The stage was at one or two days prior to W0. (B) Cocoon colors of the transgenic lines and nontransgenic strains. For nontransgenic strains, the genotypes of the *C* and the *F* genes are shown in parentheses. (C–F) Distribution of carotenoid pigmentation in the middle silk gland of the transgenic lines and nontransgenic strains during the last larval instar. The later and larger silk gland is shown on the right in each panel. (G) Representative charts of the reverse-phase HPLC analysis of carotenoid composition of the middle silk gland in the transgenic larvae, at one or two days prior to W0. Detection was performed at 445 nm. The inset in the *Ser1-GAL4/UAS-Cameo2* line is a magnification near the  $\beta$ -carotene peak. Most peaks eluting before lutein were considered to be due to the DMSO used for carotenoid extraction. (H–J) Lutein and  $\beta$ -carotene concentration in the hemolymph (H), the middle silk gland (I), and cocoons (J) (mean, SE; n = 3–5 individuals). The stage of the hemolymph and the middle silk gland was at one or two days prior to W0, except for strains c10 (W0), c43 (W0), and w06 (W0). Statistical significance (\*  $P < 0.05$ ; \*\*  $P < 0.01$ ; \*\*\*  $P < 0.00005$ ) was analyzed using Student *t*-test. The cocoon color of strain w06 (+<sup>C</sup>/<sub>C</sub>, +<sup>F</sup>/<sub>F</sub>) is shown in Fig. 1C. The late and bigger silk gland images in (C) and (E) are the same as those in Fig. 1C. Scale bar: 1 cm.



From the enhancement of selective  $\beta$ -carotene uptake into the middle silk gland and cocoons, we conclude that the *F* allele encodes *SCRB15*.

## DISCUSSION

Regardless of the essential roles of carotenoids in animals, handling of carotenoids in the body requires special processes due to its water insolubility. The molecular events involved in the transport of any carotenoid from the gut lumen to the gut epithelial cells, to the blood, and to its target cells are not yet understood. In *B. mori*, several mutants with altered cocoon colors are defective in one of the steps involved in the transport of carotenoids from the midgut lumen to its target tissue (the middle silk gland). We have been characterizing carotenoid transport at the molecular level using the *B. mori* cocoon color mutants (12, 17).

In this study, we identified the *F* gene responsible for control of the selective cellular uptake of  $\beta$ -carotene as *SCRB15*, following the identification of the *C* gene that controls selective cellular uptake of lutein (17). A homology search revealed that *SCRB15* belongs to the *CD36* gene family, which includes *Cameo2*, encoded by the *C* gene. Functional differentiation after gene duplication therefore likely facilitated differences in selectivity for carotenoid species. To date, it has been shown that members of the *CD36* family are critical for a large variety of biological activities in species from mammals to insects: these activities include angiogenesis, viral and bacterial recognition by the immune system, transport of lipids from cholesteryl ester to fatty acids, and taste and olfactory perception (42). Our study indicates that this family is also critical for discrimination of chemical structures that differ only marginally, such as carotenoids in the silkworm (Fig. 1).

A recent report indicated that the mammalian *CD36* was involved in both lycopene and lutein uptake by adipocytes (43). *CD36* homologs may not always discriminate among carotenoid species strictly.


Carotenoids are carried in the hemolymph by lipophorin, a high-density lipoprotein in insects, which contains both  $\beta$ -carotene and lutein (11). As lipophorin contains both carotenoids in its hydrophobic core, transfer of  $\beta$ -carotene or lutein from lipophorin to the middle silk gland occurs at the interface between hemolymph and cell membrane of the middle silk gland. Consistent with the emerging view, *SCRB15* and *Cameo2* are transmembrane proteins expressed in the middle silk gland. We expect that *SCRB15* and *Cameo2* function as noninternalizing lipophorin receptors that facilitate selective uptake of carotenoids, as shown for *SR-BI* for cellular uptake of cholesteryl ester from high-density lipoproteins (18).

Expression profiles of *SCRB11* and *SCRB12* were similar to that of *SCRB15* (Fig. 3C). Although the *SCRB15* mutation is apparently a main cause of  $\beta$ -carotene deficiency of the *F* mutant, it could be possible that *SCRB11* and *SCRB12*

are involved in the cellular uptake of  $\beta$ -carotene. Furthermore, this study does not exclude the possibility that the four nonsynonymous substitutions in *SCRB11*, observed between strain *c44* (*F/F*) and strain *w06* ( $+^F/+^F$ ), were a cause of the modest rescue in  $\beta$ -carotene accumulation by transgenic expression of *SCRB15* (Fig. 6).

$\beta$ -carotene is absorbed into the midgut and transferred into the hemolymph irrespective of which allele of the *F* gene is present. Considering the genomic disruption of a coding exon in the  $+^F$  allele (Fig. 4) and the middle silk gland-specific expression pattern (Fig. 3C), *SCRB15* may not be essential for absorption of  $\beta$ -carotene in the midgut. Thus, the  $\beta$ -carotene transport system in the midgut is likely to be different from that in the middle silk gland.

Selective transport of lipids other than carotenoids also occurs in insects. For example, diacylglycerol is transported by lipophorin to the flight muscle to provide an energy source for flight (44). As *CD36* family members are engaged in cellular uptake of lipids other than carotenoids in mammals, such as fatty acids or cholesteryl ester (42), it is interesting to consider the possibility that these molecules in silkworm are also involved in the transport of lipids other than carotenoids. Identification of *SCRB15* as the *F* gene casts a spotlight on this possibility for group 1 (Fig. 5B), since the function of the group 1 insect proteins remains largely unknown. It should be noted that although the *SCRB13* expression was barely detected in the tissues used in this study (Fig. 3C–E), an *SCRB13* EST clone (accession number: AK385087) was found in the corpora allata in the larvae, where juvenile hormone, an ecdysteroid hormone that is critical for insect development, is synthesized and secreted (45).

The molecular mechanism underlying the specific carotenoid selectivity of *SCRB15* and *Cameo2* is a subject for further study. While it is unknown whether the interaction between carotenoids and these proteins is direct or indirect (i.e., needing unidentified cofactors), the coding sequence of *SCRB15* should contain key residues facilitating the selectivity for  $\beta$ -carotene that would not be present in *Cameo2*, as the selectivity for carotenoids was observed by transgenic expression using the same *Ser1-GAL4* driver (Figs. 6G–J). Because production of transgenic larvae is not suitable for high-throughput studies, in vitro reconstitution of selective carotenoid uptake by *SCRB15* and *Cameo2*, such as has been achieved for cellular cholesteryl ester uptake by *SR-BI* (46–48), is required to examine the selectivity mechanism by point mutagenesis or analysis of chimeric genes of *SCRB15* and *Cameo2*.

The authors thank the members of the Insect Genome Research Unit at the National Institute of Agrobiological Sciences (Japan) for technical assistance in the sampling of *BF1* individuals for mapping; Akitoshi Kitamura and Yuri Ooi (Fuji Chemical Industry Co., Ltd.) for technical support and advice on the HPLC analysis of carotenoids; Yumiko Nakajima for providing samples of genomic DNA from *B. mandarina*; Robert O. Ryan for critical reading of the manuscript; and Atsushi Kato, Hirofumi Fujimoto, and Naoko Honda for support.

## REFERENCES

- Landrum, J. T., editor. 2009. Carotenoids: Physical, Chemical, and Biological Functions and Properties. CRC Press, Boca Raton, FL.
- Moran, N. A., and T. Jarvik. 2010. Lateral transfer of genes from fungi underlies carotenoid production in aphids. *Science*. **328**: 624–627.
- Reboul, E., and P. Borel. 2011. Proteins involved in uptake, intracellular transport and basolateral secretion of fat-soluble vitamins and carotenoids by mammalian enterocytes. *Prog. Lipid Res.* **50**: 388–402.
- Borel, P. 2012. Genetic variations involved in interindividual variability in carotenoid status. *Mol. Nutr. Food Res.* **56**: 228–240.
- Harrison, E. H. 2012. Mechanisms involved in the intestinal absorption of dietary vitamin A and provitamin A carotenoids. *Biochim. Biophys. Acta*. **1821**: 70–77.
- von Lintig, J. 2010. Colors with functions: elucidating the biochemical and molecular basis of carotenoid metabolism. *Annu. Rev. Nutr.* **30**: 35–56.
- von Lintig, J. 2012. Metabolism of carotenoids and retinoids related to vision. *J. Biol. Chem.* **287**: 1627–1634.
- Landrum, J. T., and R. A. Bone. 2001. Lutein, zeaxanthin, and the macular pigment. *Arch. Biochem. Biophys.* **385**: 28–40.
- Vachali, P., B. Li, K. Nelson, and P. S. Bernstein. 2012. Surface plasmon resonance (SPR) studies on the interactions of carotenoids and their binding proteins. *Arch. Biochem. Biophys.* **519**: 32–37.
- Nakajima, M. 1963. Physiological studies on the function of genes concerning carotenoid permeability in the silkworm. *Bull. Fac. Agric. Tokyo Univ. Agric. Technol.* **1**: 1–80.
- Tsuchida, K., M. Arai, Y. Tanaka, R. Ishihara, R. O. Ryan, and H. Maekawa. 1998. Lipid transfer particle catalyzes transfer of carotenoids between lipophorins of *Bombyx mori*. *Insect Biochem. Mol. Biol.* **28**: 927–934.
- Sakudoh, T., and K. Tsuchida. 2009. Transport of carotenoids by a carotenoid-binding protein in the silkworm. In *Carotenoids: Physical, Chemical, and Biological Functions and Properties*. J. T. Landrum, editor. CRC Press, Boca Raton, FL. 511–523.
- Tazima, Y. 1964. The Genetics of the Silkworm. Logos Press, UK.
- Ishii, K. 1917. On a yellow blood and white cocoon mutant of the silkworm. *Sakurakai Zasshi*. **1**: 113–115.
- Uda, H. 1919. On the relation between blood colour and cocoon colour in the silkworm, with special reference to Mendel's law of heredity. *Genetics*. **4**: 395–416.
- Cleghorn, M. L. 1918. First report on the inheritance of visible and invisible characters in silkworms. *Proc. Zool. Soc. Lond.* **88**: 133–146.
- Sakudoh, T., T. Iizuka, J. Narukawa, H. Sezutsu, I. Kobayashi, S. Kuwazaki, Y. Banno, A. Kitamura, H. Sugiyama, N. Takada, et al. 2010. A CD36-related transmembrane protein is coordinated with an intracellular lipid-binding protein in selective carotenoid transport for cocoon coloration. *J. Biol. Chem.* **285**: 7739–7751.
- Rigotti, A., and M. Krieger. 2010. The HDL receptor SR-BI. In *High Density Lipoproteins, Dyslipidemia, and Coronary Heart Disease*. E. J. Schaefer, editor. Springer, New York. 103–109.
- Yamamoto, K., J. Nohata, K. Kadono-Okuda, J. Narukawa, M. Sasanuma, S. I. Sasanuma, H. Minami, M. Shimomura, Y. Suetsugu, Y. Banno, et al. 2008. A BAC-based integrated linkage map of the silkworm *Bombyx mori*. *Genome Biol.* **9**: R21.
- Shimomura, M., H. Minami, Y. Suetsugu, H. Ohyanagi, C. Satoh, B. Antonio, Y. Nagamura, K. Kadono-Okuda, H. Kajiwara, H. Sezutsu, et al. 2009. KAIKObase: an integrated silkworm genome database and data mining tool. *BMC Genomics*. **10**: 486.
- Niwa, R., T. Sakudoh, T. Namiki, K. Saida, Y. Fujimoto, and H. Kataoka. 2005. The ecdysteroidogenic P450 Cyp302a1/disembodied from the silkworm, *Bombyx mori*, is transcriptionally regulated by prothoracicotropic hormone. *Insect Mol. Biol.* **14**: 563–571.
- The International Silkworm Genome Consortium. 2008. The genome of a lepidopteran model insect, the silkworm *Bombyx mori*. *Insect Biochem. Mol. Biol.* **38**: 1036–1045.
- Koike, Y., K. Mita, M. G. Suzuki, S. Maeda, H. Abe, K. Osoegawa, P. J. deJong, and T. Shimada. 2003. Genomic sequence of a 320-kb segment of the Z chromosome of *Bombyx mori* containing a kettin ortholog. *Mol. Genet. Genomics*. **269**: 137–149.
- Mita, K., M. Kasahara, S. Sasaki, Y. Nagayasu, T. Yamada, H. Kanamori, N. Namiki, M. Kitagawa, H. Yamashita, Y. Yasukochi, et al. 2004. The genome sequence of silkworm, *Bombyx mori*. *DNA Res.* **11**: 27–35.
- Sakudoh, T., K. Tsuchida, and H. Kataoka. 2005. BmStart1, a novel carotenoid-binding protein isoform from *Bombyx mori*, is orthologous to MLN64, a mammalian cholesterol transporter. *Biochem. Biophys. Res. Commun.* **336**: 1125–1135.
- Imamura, M., J. Nakai, S. Inoue, G. X. Quan, T. Kanda, and T. Tamura. 2003. Targeted gene expression using the GAL4/UAS system in the silkworm *Bombyx mori*. *Genetics*. **165**: 1329–1340.
- Sakudoh, T., H. Sezutsu, T. Nakashima, I. Kobayashi, H. Fujimoto, K. Uchino, Y. Banno, H. Iwano, H. Maekawa, T. Tamura, et al. 2007. Carotenoid silk coloration is controlled by a carotenoid-binding protein, a product of the Yellow blood gene. *Proc. Natl. Acad. Sci. USA*. **104**: 8941–8946.
- Tamura, T., C. Thibert, C. Royer, T. Kanda, E. Abraham, M. Kamba, N. Komoto, J. L. Thomas, B. Mauchamp, G. Chavancy, et al. 2000. Germline transformation of the silkworm *Bombyx mori* L. using a piggyBac transposon-derived vector. *Nat. Biotechnol.* **18**: 81–84.
- Tatematsu, K., I. Kobayashi, K. Uchino, H. Sezutsu, T. Iizuka, N. Yonemura, and T. Tamura. 2010. Construction of a binary transgenic gene expression system for recombinant protein production in the middle silk gland of the silkworm *Bombyx mori*. *Transgenic Res.* **19**: 473–487.
- Simodaira, M. 1947. Studies of linkage in the silkworm. I. Relation between VI and VIII linkage group. *Jpn. J. Genet.* **22**: 82–84.
- Banno, Y., K. Sakaida, T. Nakamura, K. Tsuchida, Y. Kawaguchi, K. Koga, and H. Doira. 1997. Reassessment of mapping of the E homeotic gene complex of *Bombyx mori* by linkage analysis and in situ hybridization with an Antennapedia clone as a probe. *J. Seric. Sci. Jap.* **66**: 151–155.
- Osanaï-Futahashi, M., Y. Suetsugu, K. Mita, and H. Fujiwara. 2008. Genome-wide screening and characterization of transposable elements and their distribution analysis in the silkworm, *Bombyx mori*. *Insect Biochem. Mol. Biol.* **38**: 1046–1057.
- Goldsmith, M. R. 2009. Recent progress in silkworm genetics and genomics. In *Molecular Biology and Genetics of the Lepidoptera*. M. R. Goldsmith and F. Marec, editors. CRC Press, Boca Raton, FL. 25–48.
- Xia, Q., Y. Guo, Z. Zhang, D. Li, Z. Xuan, Z. Li, F. Dai, Y. Li, D. Cheng, R. Li, et al. 2009. Complete resequencing of 40 genomes reveals domestication events and genes in silkworm (*Bombyx*). *Science*. **326**: 433–436.
- Sonnhammer, E. L., G. von Heijne, and A. Krogh. 1998. A hidden Markov model for predicting transmembrane helices in protein sequences. *Proc. Int. Conf. Intell. Syst. Mol. Biol.* **6**: 175–182.
- Hoosdally, S. J., E. J. Andress, C. Wooding, C. A. Martin, and K. J. Linton. 2009. The Human Scavenger Receptor CD36: glycosylation status and its role in trafficking and function. *J. Biol. Chem.* **284**: 16277–16288.
- Petersen, T. N., S. Brunak, G. von Heijne, and H. Nielsen. 2011. SignalP 4.0: discriminating signal peptides from transmembrane regions. *Nat. Methods*. **8**: 785–786.
- Zhan, S., C. Merlin, J. L. Boore, and S. M. Reppert. 2011. The monarch butterfly genome yields insights into long-distance migration. *Cell*. **147**: 1171–1185.
- Nichols, Z., and R. G. Vogt. 2008. The SNMP/CD36 gene family in Diptera, Hymenoptera and Coleoptera: *Drosophila melanogaster*, *D. pseudoobscura*, *Anopheles gambiae*, *Aedes aegypti*, *Apis mellifera*, and *Tribolium castaneum*. *Insect Biochem. Mol. Biol.* **38**: 398–415.
- Vogt, R. G., N. E. Miller, R. Litvack, R. A. Fandino, J. Sparks, J. Staples, R. Friedman, and J. C. Dickens. 2009. The insect SNMP gene family. *Insect Biochem. Mol. Biol.* **39**: 448–456.
- Tsuchida, K., Z. E. Jouni, J. Gardetto, Y. Kobayashi, H. Tabunoki, M. Azuma, H. Sugiyama, N. Takada, H. Maekawa, Y. Banno, et al. 2004. Characterization of the carotenoid-binding protein of the Y-gene dominant mutants of *Bombyx mori*. *J. Insect Physiol.* **50**: 363–372.
- Silverstein, R. L., and M. Febbraio. 2009. CD36, a scavenger receptor involved in immunity, metabolism, angiogenesis, and behavior. *Sci. Signal.* **2**: re3.
- Moussa, M., E. Gouranton, B. Gleize, C. E. Yazidi, I. Niot, P. Besnard, P. Borel, and J. F. Landrier. 2011. CD36 is involved in lycopene and lutein uptake by adipocytes and adipose tissue cultures. *Mol. Nutr. Food Res.* **55**: 578–584.
- Ryan, R. O., and D. J. Van der Horst. 2011. Lipid transport. In *Insect Molecular Biology and Biochemistry*. L. I. Gilbert, editor. Academic Press, Waltham, MA. 317–345.
- Daimon, T., T. Kozaki, R. Niwa, I. Kobayashi, K. Furuta, T. Namiki, K. Uchino, Y. Banno, S. Katsuma, T. Tamura, et al. 2012. Precocious

- metamorphosis in the juvenile hormone-deficient mutant of the silkworm, *Bombyx mori*. *PLoS Genet.* **8**: e1002486.
46. Papale, G. A., K. Nicholson, P. J. Hanson, M. Pavlovic, V. A. Drover, and D. Sahoo. 2010. Extracellular hydrophobic regions in scavenger receptor BI play a key role in mediating HDL-cholesterol transport. *Arch. Biochem. Biophys.* **496**: 132–139.
  47. Hu, J., Z. Zhang, W. J. Shen, A. Nomoto, and S. Azhar. 2011. Differential roles of cysteine residues in the cellular trafficking, dimerization, and function of the high-density lipoprotein receptor, SR-BI. *Biochemistry.* **50**: 10860–10875.
  48. Nieland, T. J., S. Xu, M. Penman, and M. Krieger. 2011. Negatively cooperative binding of high-density lipoprotein to the HDL receptor SR-BI. *Biochemistry.* **50**: 1818–1830.
  49. Tanaka, H., J. Ishibashi, K. Fujita, Y. Nakajima, A. Sagisaka, K. Tomimoto, N. Suzuki, M. Yoshiyama, Y. Kaneko, T. Iwasaki, et al. 2008. A genome-wide analysis of genes and gene families involved in innate immunity of *Bombyx mori*. *Insect Biochem. Mol. Biol.* **38**: 1087–1110.
  50. Sakudoh, T., T. Nakashima, Y. Kuroki, A. Fujiyama, Y. Kohara, N. Honda, H. Fujimoto, T. Shimada, M. Nakagaki, Y. Banno, et al. 2011. Diversity in copy number and structure of a silkworm morphogenetic gene as a result of domestication. *Genetics.* **187**: 965–976.
  51. Tamura, K., D. Peterson, N. Peterson, G. Stecher, M. Nei, and S. Kumar. 2011. MEGA5: molecular evolutionary genetics analysis using maximum likelihood, evolutionary distance, and maximum parsimony methods. *Mol. Biol. Evol.* **28**: 2731–2739.
  52. Pelletier, J., F. Bozzolan, M. Solvar, M. C. Francois, E. Jacquinjoly, and M. Maibeche-Coisne. 2007. Identification of candidate aldehyde oxidases from the silkworm *Bombyx mori* potentially involved in antennal pheromone degradation. *Gene.* **404**: 31–40.
  53. Rogers, M. E., M. Sun, M. R. Lerner, and R. G. Vogt. 1997. Snmp-1, a novel membrane protein of olfactory neurons of the silk moth *Antheraea polyphemus* with homology to the CD36 family of membrane proteins. *J. Biol. Chem.* **272**: 14792–14799.
  54. Benton, R., K. S. Vannice, and L. B. Vosshall. 2007. An essential role for a CD36-related receptor in pheromone detection in *Drosophila*. *Nature.* **450**: 289–293.
  55. Jin, X., T. S. Ha, and D. P. Smith. 2008. SNMP is a signaling component required for pheromone sensitivity in *Drosophila*. *Proc. Natl. Acad. Sci. USA.* **105**: 10996–11001.